Plant Science 330 (2023) 111638

Contents lists available at ScienceDirect

Plant Science

journal homepage: www.elsevier.com/locate/plantsci

SlGH3.15, a member of the *GH3* gene family, regulates lateral root development and gravitropism response by modulating auxin homeostasis in tomato

Guo Ai [a,1], Rong Huang [a,1], Dedi Zhang [a], Miao Li [a], Guobin Li [a], Wangfang Li [a], John K. Ahiakpa [a], Yikui Wang [b], Zonglie Hong [c], Junhong Zhang [a,*]

[a] National Key Laboratory for Germplasm Innovation and Utilization of Horticultural Crops, Huazhong Agricultural University, Wuhan, Hubei, 430070, China
[b] Vegetable Research Institute, Guangxi Academy of Agricultural Sciences, Nanning, Guangxi, 530007, China
[c] Department of Plant Sciences, University of Idaho, Moscow, ID 83844, USA

ARTICLE INFO

Keywords:
Auxin
Hormonal homeostasis
Solanum lycopersicum
Root formation
GH3 gene

ABSTRACT

Multiple *Gretchen Hagen 3* (*GH3*) genes have been implicated in a range of processes in plant growth and development through their roles in maintaining hormonal homeostasis. However, there has only been limited study on the functions of *GH3* genes in tomato (*Solanum lycopersicum*). In this work, we investigated the important function of *SlGH3.15*, a member of the *GH3* gene family in tomato. Overexpression of *SlGH3.15* led to severe dwarfism in both the above- and below-ground sections of the plant, accompanied by a substantial decrease in free IAA content and reduction in the expression of *SlGH3.9*, a paralog of *SlGH3.15*. Exogenous supply of IAA negatively affected the elongation of the primary root and partially restored the gravitropism defects in *SlGH3.15*-overexpression lines. While no phenotypic change was observed in the *SlGH3.15* RNAi lines, double knockout lines of *SlGH3.15* and *SlGH3.9* were less sensitive to treatments with the auxin polar transport inhibitor. Overall, these findings revealed important roles of *SlGH3.15* in IAA homeostasis and as a negative regulator of free IAA accumulation and lateral root formation in tomato.

1. Introduction

Roots, an important plant organ, play vital roles in providing the aerial portions of the plant for structural support, water and nutrient uptake, and adaptation to the changing environment (Osmont et al., 2007; Petricka et al., 2012). The formation of lateral roots has been widely studied, especially in the model plant *Arabidopsis* (Petricka et al., 2012). It has been postulated that there are four main stages in lateral root formation, encompassing the priming, initiation, primordium development, and emergence of lateral roots (Peret et al., 2009). A rich set of literature over the past several decades has documented that auxin has crucial functions in root emergence and development (Vanneste and Friml, 2009). During the early seedling development, indole-3-acetic acid (IAA) concentrations in root tips have significant impacts on the timing of lateral root emergence in *Arabidopsis* (Bhalerao et al., 2002). Loss of function of the *Arabidopsis PIN-FORMED* 4 (*AtPIN4*) has been shown to fail to maintain endogenous auxin levels, resulting in morphological defects on roots (Friml et al., 2002). Increased expression of *PIN3* and *PIN7* has been demonstrated to improve auxin transport and reduce localized auxin accumulation, leading to inhibition of lateral root development (Lewis et al., 2011). The *transparent testa4* (tt4) mutant plants of *Arabidopsis* exhibit changes in auxin transport and response of roots to gravity and light (Buer and Muday, 2005). It has been shown that induced expression of the B19 auxin transporter increases IAA accumulation and enhances adventitious root formation (Sukumar et al., 2013). Auxin-inducible *IAA12* or *IAA13* could prevent ARF5-dependent embryonic root formation (Weijers et al., 2005). Different mechanisms, especially for auxin roles, comprising auxin biosynthesis, transport, and auxin signaling, have been proposed to control lateral root formation in plants.

Auxin, as a vital hormone, is well known to regulate root formation, development and response to environmental stress (Vanneste and Friml, 2009). Auxin was first identified in 1880 by Charles Darwin (Woodward and Bartel, 2005). Among many natural and synthetic chemicals

* Corresponding author.
E-mail address: zhangjunhng@mail.hzau.edu.cn (J. Zhang).
[1] These authors contributed equally

https://doi.org/10.1016/j.plantsci.2023.111638
Received 29 November 2022; Received in revised form 26 January 2023; Accepted 11 February 2023
Available online 15 February 2023

exhibiting auxin-like activities, IAA is recognized to be the most widespread auxin in plants (Woodward and Bartel, 2005; Korasick et al., 2013). Excessive or insufficient accumulations of auxin hinders plant growth and development (Staswick et al., 2005). Based on the participation of the amino acid tryptophan (Trp), IAA biosynthesis in plants is classified into Trp-dependent and Trp-independent pathways (Mashiguchi et al., 2011; Zhao, 2012). The Trp-dependent route can be divided into several pathways, depending on the involvement of key intermediates, including indole-3-acetamide (IAM), indole-3-acetaldoxime (IAOx), indole-3-pyruvic acid (IPyA) (Zhao, 2012). Among the Trp-dependent pathways, the IPyA route is the primary source of IAA content in plants (Stepanova et al., 2011; Won et al., 2011). In the IPyA pathway, tryptophan aminotransferases (TAA1) and YUCCA flavin monooxygenases (YUC1) are the two enzymes responsible for catalyzing the IPyA and IAA conversions. Those two enzymes and the pathways are conserved throughout the plants (Stepanova et al., 2008; Ishida et al., 2016). YUC1 encodes a flavin monooxygenase (FMO) that has been shown to be a rate-limiting enzyme in a Trp-dependent auxin biosynthesis pathway (Exposito-Rodriguez et al., 2007). The IAM pathway is bacteria-specific in the IAA biosynthesis (Mano and Nemoto, 2012), and IAM serves as an intermediary for conversion of IAOx to IAA (Sugawara et al., 2009). It has been demonstrated that tryptophan decarboxylase (TDC) and several YUCCA proteins involved in the TAM pathway can also convert Trp to IAA (Mano and Nemoto, 2012). Also, *TDC* and *YUCCA* genes have been identified in many plants (Mano and Nemoto, 2012). However, the IAOx pathway is considered to be plant species-specific.

Furthermore, IAA can be synthesized in young tissues and organs, including leaves, cotyledons, roots, and seedlings. Younger leaves possess the highest IAA biosynthetic capacity in *Arabidopsis* (Ljung et al., 2001). Apart from the auxin synthesis, auxin homeostasis is also important in plants. In general, after IAA is synthesized in plants, it may either be catabolized, conjugated, or transported to other tissues to maintain the right levels for different physiological processes (Korasick et al., 2013). Excess IAA could be deactivated through several ways, including conjugation with sugars and amino acids, transportation to other tissues, degradation, and oxidation (Ludwig-Mueller, 2011).

As one of the important primary early auxin-responsive gene families, the *GH3* family contains several members that are known to participate in the conjugation of amino acids or glucose to a number of phytohormones (Ludwig-Mueller, 2011; Staswick et al., 2002). The first *GH3* gene was identified in soybean through screening of auxin-responsive genes after auxin treatments (Hagen and Guilfoyle, 2002). Members of the *GH3* gene family are divvied into three subgroups (I, II, and III) and several members have been documented to play a crucial role in regulating the intracellular auxin level in plants (Okrent and Wildermuth, 2011). It has been reported that the IAA conjugation reactions are catalyzed by enzymes of the GH3 family. They can modulate phytohormone actions and their roles in a series of biological pathways have been characterized and implicated over the past decades (Chen et al., 2010). A *GH3* gene in *Arabidopsis*, *Jasmonate Resistant 1* (*JAR1*) converts jasmonic acid (JA) to isoleucine and functions in the adenylation of JA, salicylic acid (SA), and IAA (Staswick et al., 2002). Overexpression of *OsGH3.1* leads to a decrease in free auxin concentration in rice (Domingo et al., 2009). Two Arabidopsis *GH3* proteins, Yadokari 1 (YDK1) and Dwarf in Light 1 (DFL1), inhibit elongation of shoot cells and lateral root development, respectively (Nakazawa et al., 2001; Takase et al., 2004). Several studies (nullK) have reported that the *AtGH3.9* gene functions in the crosstalk between auxin and JA signaling pathways to control primary root development in *Arabidopsis*. The rice GH3.8 proteins are unable to function properly without the presence of Mg^{2+} or Mn^{2+} metal ions (Chen et al., 2010). In *Capsicum chinese* L., auxin and ethylene regulate the expression of *CcGH3*, a *GH3*-like gene, which may accelerate ripening of ethylene-treated fruits (Liu et al., 2005). *AtGH3.5* participates in auxin and SA signaling in *Arabidopsis* during pathogen infections (Zhang et al., 2007). Additionally, *GH3* genes have been reported to be induced by cadmium in *Brassica juncea* (Minglin et al., 2005). In grape berry and longan, *GH3* genes have been recently shown to play roles in fruits ripening (Kuang et al., 2011; Boettcher et al., 2010). Three *GH3* genes (*AtGH3.3*, *AtGH3.5*, and *AtGH3.6*) in *Arabidopsis thaliana* are responsible for fine-tuning adventitious root development by mediating jasmonate homeostasis (Gutierrez et al., 2012). Although important and complex functions of *GH3* genes are identified, more studies are needed to be conducted to fully explore the roles of *GH3* genes in plant development.

In the tomato genome, there are 15 *GH3* genes (*SlGH3.1* - *SlGH3.15*) (Kumar et al., 2012), which can be grouped into two distinct categories: Group I and Group II. Group I contains nine genes (Liao et al., 2015). The remaining six *SlGH3* genes belong to Group II, and are induced by IAA (Kumar et al., 2012). It is interesting to note that *SlGH3.4* in Group I is highly responsive to arbuscular mycorrhizal symbiosis (Liao et al., 2015). In a recent study, nine additional *GH3* genes have been found in tomato, resulting in a total of 24 members in the *GH3* gene family (Sravankumar et al., 2018). *SlGH3.2*, induced by ripening, has influence on fruit ripening in tomato by modulating the auxin and ethylene crosstalk (Sravankumar et al., 2018). *SlGH3.8* acts downstream of *YABBY2b* to influence plant height (Sun et al., 2020). Remarkably, in the history of tomato breeding, *SlGH3.15* has been used as a significant gene for regulating tomato fruit size (Lin et al., 2014). In summary, there have been limited reports on the specific functions of *GH3* genes in tomato.

Here, we demonstrated the essential roles played by *SlGH3.15*, as well as its redundant function with other paralogs, in regulating free IAA produced in tomato. Dwarfism and significant changes in root growth and development, including the production of short roots, suppression of lateral roots, and absence of gravitropism were manifest in plants with elevated *SlGH3.15* expression. It was shown that *SlGH3.15*-overexpression (*SlGH3.15*-OE) lines were less sensitive to exogenous IAA. Double knockout lines of *SlGH3.15* and *SlGH3.9* through CRISPR/Cas9 produced more lateral roots and were less sensitive to exogenous naphthylphthalamic acid (NPA) treatment.

2. Results

2.1. Expression pattern of SlGH3.15 and subcellular localization of its protein

The genomic DNA region of *SlGH3.15* comprises three exons and two introns, and the cDNA for this gene has a reading frame of 1830 bp in length, which encodes a polypeptide of 609 amino acids (Fig. 1A). From the gene expression result, *SlGH3.15* was highly expressed in the root, leaf, and flower tissues, but weakly expressed in the stems and ripening fruits (Fig. 1B). These findings indicate that *SlGH3.15* expression was more abundantly in the vegetative tissues than in reproductive tissues, and suggest that *SlGH3.15* plays a crucial role in the vegetative growth. SlGH3.15 protein is predicted to be a member of the GH3 Group II. We constructed a phylogenetic tree using the protein sequences of the GH3 family, created by the neighbor-joining method. Analysis of the phylogenetic tree revealed that SlGH3.9 shared the highest sequence similarity with SlGH3.15 (Fig. 1C).

To further study the function of *SlGH3.15*, we analyzed the subcellular localization of its protein product. Tobacco (*Nicotiana benthamiana*) leaves were transiently transfected to express a fusion protein composed of *SlGH3.15* and yellow fluorescent protein (*SlGH3.15*-YFP). The results (Fig. 1D) showed that the yellow fluorescence signal was detected in both the nucleus and cytoplasm.

2.2. Overexpression of SlGH3.15 leads to abnormal morphology in tomato

Through the use of the constitutive promoter CaMV35S, *SlGH3.15* was overexpressed in transgenic tomato and the relative expression levels of *SlGH3.15* in leaves of the overexpression lines OE-10, OE-12, and OE-24 were over 200-fold greater than in the control AC leaves

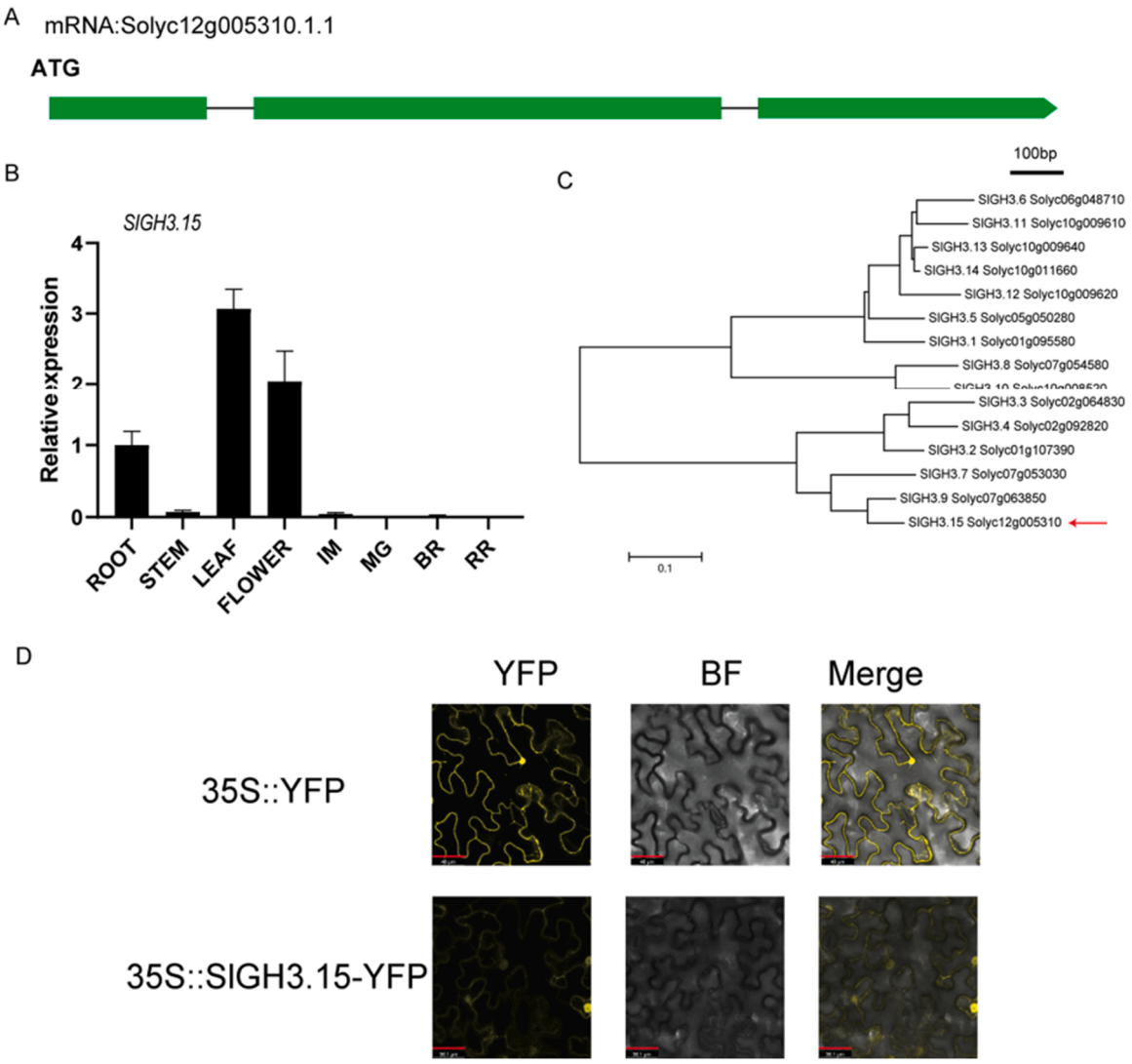

Fig. 1. Molecular characterization of *SlGH3.15*. (**A**) Genomic DNA structure of *SlGH3.15*. Exons are shown in thick green lines, whereas introns are shown in thin black lines. (**B**) Gene expression patterns of *SlGH3.15* in different organs (root, stem, leaf, flower, and fruits) of tomato. Fruits were collected for gene expression analysis from different maturity stages including the immature green (IM), mature green (MG), breaker (BR), and red ripe (RR). Following total RNA isolation, relative expression analysis (n = 3) was performed using quantitative real-time PCR (qRT-PCR). Mean standard deviations (SD) are shown for data collected from three independent samples. (**C**) Phylogenetic tree of GH3 proteins was created by the neighbor-joining method. The scale bar corresponds to 0.1 amino acid substitutions per residue. The red arrow points to the SlGH3.15 sequence. (D) Subcellular localization of SlGH3.15-YFP fusion protein in *N. banthamiana* leaves. YFP, yellow fluorescent protein. Images were taken under bright-light field (BF) or using a microscopic filter for YFP. Bars: 48 μm (top panel), 36.1 μm (bottom panel).

(Fig. 2A-B). Using RNA interference (RNAi), we also produced transgenic plants with reduced *SlGH3.15* expression in the AC genomic background. After obtaining 11 RNAi transgenic plants, we found that *SlGH3.15* transcript levels were lower in three typical RNAi lines (R-16, R-17, and R-39) compared to the control AC (Fig. 2A-B).

SlGH3.15-OE lines exhibited aberrant morphologies such as smaller, crinklier leaves, slowed growth, and altered plant architecture (Fig. 2A–D). Plant height and internodal length were also significantly different between *SlGH3.15*-OE lines and the control group (Fig. 2E). *SlGH3.15*-OE lines were found to have a smaller number of lateral roots and shorter main roots compared to the control plants AC. There was a statistically significant difference ($p < 0.01$) between the two groups (Fig. 2F–G). However, in contrast to AC, no substantial phenotypic changes were observed in the *SlGH3.15*-RNAi lines (Fig. 2). Taken together, it was hypothesized that *SlGH3.15* and its paralogs in the *GH3* gene family may play redundant functions in tomato.

We selected two lines (*SlGH3.15*-OE-10 and *SlGH3.15*-R-16 lines) as representatives for overexpression and suppressed lines, respectively, to study the difference in root growth between the transgenic lines and the AC control. The seeds were germinated on 1/2 MS-agar culture media. The results indicated that seedlings of *SlGH3.15*-OE-10 showed root agravitropism (Fig. 3A), few lateral roots (Fig. 3B), and shorter main roots (Fig. 3C) as compared to the control plants 14 days post germination (Fig. 3). These findings uncovered crucial functions for *SlGH3.15*, including those in root gravitropism, plant development, and lateral root formation. In contrast, root growth and gravitropism were unaffected in RNAi-seedlings (Fig. 3), indicating possible redundancy of *SlGH3.15* in tomato.

2.3. *Overexpression of SlGH3.15 reduces free IAA accumulation*

GH3 genes have been implicated in the conjugation of amino acids or glucose to various phytohormones (Gutierrez et al., 2012). In this study, IAA-deficient phenotypes were recorded in the *GH3.15* overexpression lines (Fig. 2). We analyzed free IAA in *SlGH3.15*-OE and RNAi lines. When compared to the wild type AC control, the amount of free IAA in

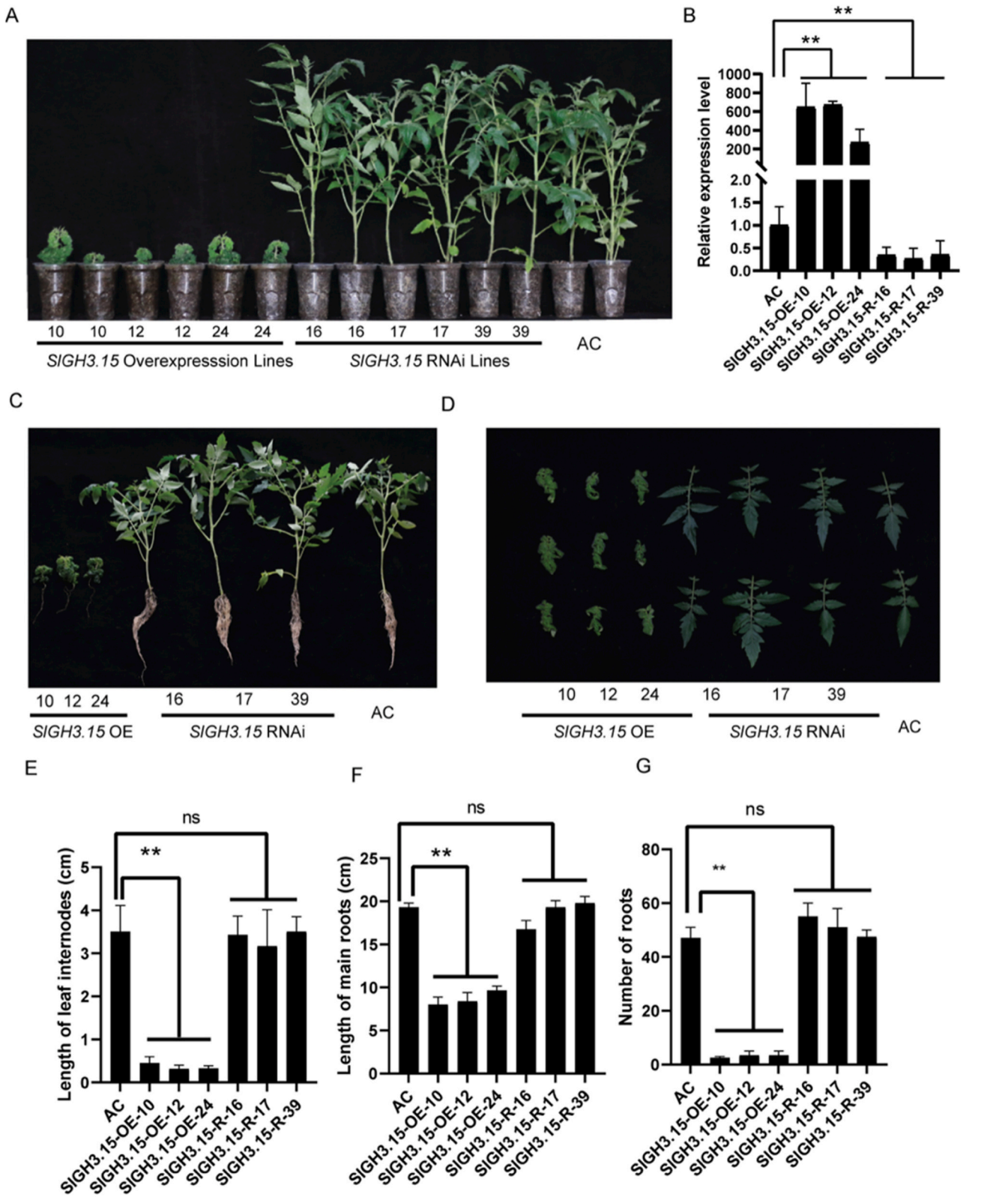

Fig. 2. Morphology of transgenic tomato plants with altered expression of *SlGH3.15*. (A) 4-week-old seedlings of *SlGH3.15*-OE lines, *SlGH3.15*-RNAi lines, and AC plants grown in a green house. (B) Relative expression levels of the *SlGH3.15* transcripts in *SlGH3.15*-OE and *SlGH3.15*-RNAi lines in comparison with the AC control. The expression level of *SlGH3.15* in AC was set as 1.0. Shown are means with standard errors (n = 3). (C) Roots of 4-week-old seedlings of *SlGH3.15*-OE lines, *SlGH3.15*-RNAi lines, and AC plants. (D) Immature leaves from *SlGH3.15*-OE lines, *SlGH3.15*-RNAi lines, and AC plants. (E) Average length (cm) of leaf internodes in 4-week-old seedlings. (F) Length of main roots (cm) in 4-week-old seedlings (n = 10). (G) Number of roots in 4-week-old seedlings (n = 10). The asterisks indicate level of significance between groups. *, $P < 0.05$; **, $P < 0.01$; ns, no significant.

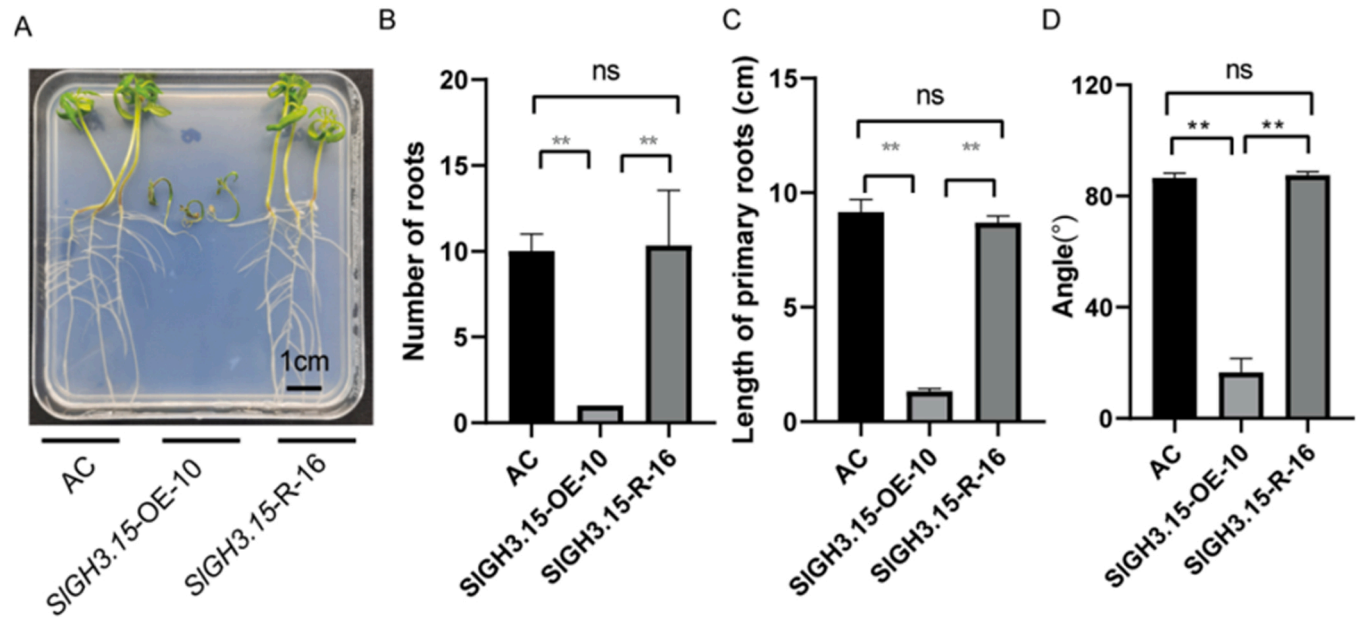

Fig. 3. Root architecture of transgenic tomato plants with altered expression of *SlGH3.15*. (A) 12-day-old seedlings of *SlGH3.15*-OE lines and AC plants grown in ½MS-agar culture medium. Scale bar, 1 cm. (B) Number of roots in the seedlings (n = 3). (C) Length of primary roots (cm) in the seedlings (n = 3). (D) Angles of root apices along the gravity in transgenic lines and AC control. Angles of root apices were defined as the angles between the horizontal line and the line from the root base towards the root apex (see Fig. S5). The asterisks indicate significant differences between groups based on Student's *t*-tests: *, $P < 0.05$; **, $P < 0.01$; ns, no significant.

SlGH3.15-OE lines was drastically lower (3 ng/g) (Fig. 4A). *SlGH3.15*-RNAi line R-16 had a slightly greater free IAA level than AC, but this was not significantly different from either of the other two RNAi lines (R-17 or R-39) (Fig. 4A). These results indicate that the decrease in endogenous free IAA was likely responsible for the phenotypic alterations observed in the transgenic *SlGH3.15*-OE lines. In contrast, *SlGH3.15* RNAi lines did not exhibit any visible growth phenotype. This led us to the proposal that a paralog of *SlGH3.15* with redundant function may exist in tomato. Four *GH3* genes (*SlGH3.2*, *SlGH3.4*, *SlGH3.7*, and *SlGH3.9*) were identified to be most closely related to *SlGH3.15* from the phylogenetic tree (Fig. 1C). The expression patterns of *SlGH3.2*, *SlGH3.4*, and *SlGH3.7* were similar between the transgenic lines and AC (Fig. S2). However, the expression of *SlGH3.9* was found to be suppressed in the *SlGH3.15*-OE lines (Fig. 4B). Meanwhile, no significant variation in relative expression of *SlGH3.9* was recorded between the *SlGH3.15*-RNAi lines (Fig. 4B) and the control AC (Fig. 4B). Taken together, these findings suggest that *SlGH3.9* and *SlGH3.15* might perform some overlapping functions in tomato.

2.4. Exogenous IAA supply rescues the geotropic defects of SlGH3.15-OE lines

To test if exogenous IAA supply could rescue the geotropic defects of roots in *SlGH3.15*-OE lines, we treated the seedlings with different IAA

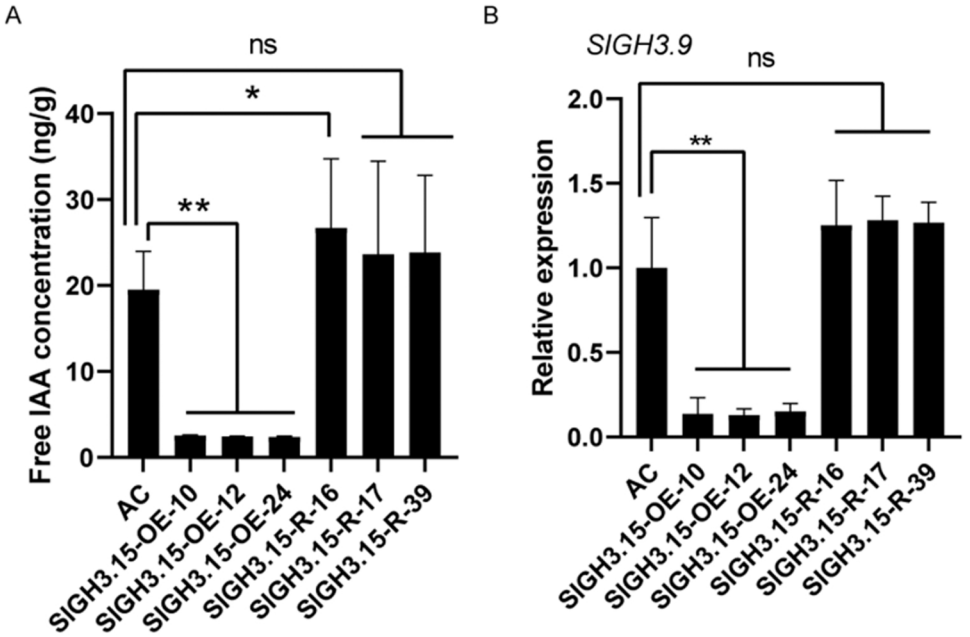

Fig. 4. Free IAA concentrations in transgenic tomato plants with altered expression of *SlGH3.15*. (A) Free IAA content (ng/g fresh leaves) in 4-week-old seedlings (n = 3). The third and fourth leaves downward from the apex were collected from the 4-week-old seedlings of transgenic lines and AC. The leaf samples were immediately frozen in liquid nitrogen and stored at −80 ℃ for free IAA content measurement. (B) Relative expression levels of the *SlGH3.9* transcripts in *SlGH3.15*-OE and *SlGH3.15*-RNAi mutants in comparison with the AC control (n = 3). The asterisks indicate significant differences between groups based on Student's *t*-tests: *, $P < 0.05$; **, $P < 0.01$; ns, no significant.

concentrations up to 1.6 mg/L. The main roots of AC were sensitive to the treatment of different IAA concentrations and became shorter as the IAA concentrations increased from 0.025 to 1.6 mg/L (Figs. 5 and S1, S2). We found that the angles of root apices along the gravity showed significant changes with different IAA concentrations treatments in *SlGH3.15*-OE lines as compared to the AC plants (Figs. 5A and S1, S3). The geotropism of root growth in *SlGH3.15*-OE lines was restored by the 0.1 mg/L IAA treatment (Fig. 5). As the IAA concentrations continued to increase from 0.4 to 1.6 mg/L, the formation of lateral roots in *SlGH3*0.15-OE lines was severely inhibited (Fig. 5). These results suggest that the exogenous IAA treatment had negative effects on root elongation in *SlGH3.15*-OE lines as in AC plants. Exogenous IAA supply at a low concentration could partially restore the phenotype of geotropism in *SlGH3.15*-OE lines. These results also suggest different IAA concentrations may have complex roles in root development, especially for the elongation of roots and initiation of lateral roots.

2.5. Effect of double knockout of SlGH3.15 and SlGH3.9 on lateral root formation

Given that *SlGH3.9* might have a potential redundant function as *SlGH3.15* in the formation of lateral roots, we generated a double mutant of *gh3.15/gh3.9* through the CRISPR/Cas9 technology to simultaneously knock out *SlGH3.15* and *SlGH3.9* in transgenic tomato plants. We generated two sgRNAs, targeting exon 2 of *SlGH3.15* and exon 2 of *SlGH3.9*, respectively (Fig. 6). We analyzed the genomic DNA sequences in the target regions in transgenic plants and found double mutant lines in which both *SlGH3.15* and *SlGH3.9* were mutated. The double mutant line *gh3.15/gh3.9*-CR-1 carried a single 1-bp insertion (G) and a single 4-bp deletion in the target region of *SlGH3.9* and *SlGH3.15*, respectively. In the double mutant line *gh3.15/gh3.9*-CR-6, one base pair (T) was inserted in the target region of *GH3.9* and a single 20-bp deletion was found in *GH3.15* (Fig. 6). In both double mutant lines (*gh3.15/gh3.9*-CR-1 and CR-6), the gene editing resulted in the frame shift in both the *SlGH3.15* and *SlGH3.9* genes.

To determine if the double mutation had any effect on root growth, we tested how the *gh3.15/gh3.9*-CR lines respond to exogenous treatment with naphthylphthalamic acid (NPA), a significant inhibitor of the polar auxin transport in plants (Teale and Palme, 2018; Abas et al., 2021). The ½ MS-agar medium containing various doses of NPA was used for seed germination of the double mutants. Root phenotypes were recorded when the plates were held at a vertical angle. When the NPA content was low (0.0825 mg/L), our data showed that the *gh3.15/gh3.9*-CR lines produced more lateral roots than the AC control. Root development in control AC plants was severely stunted by a reasonably high concentration of NPA (1 mg/L), consistent with the similar effects of the double mutation in *gh3.15/gh3.9*-CR lines on the number of lateral roots and length of roots (Figs. 7 and S4). Root development in both the AC control and *gh3.15/gh3.9*-CR lines was drastically retarded by exposure to NPA at a dosage of 16 mg/L. Furthermore, we observed root agravitropism (Fig. 7A) when plants from the *gh3.15/gh3.9*-CR lines and AC were treated with NPA, similar to the defect of root growth in the *SlGH3.15*-OE lines. This finding suggests that a lack of IAA polar transport is linked to the root agravitropism observed in the *SlGH3.15*-OE lines (Fig. 3A). Consequently, our data suggests that the *gh3.15/gh3.9*-CR double mutants were more

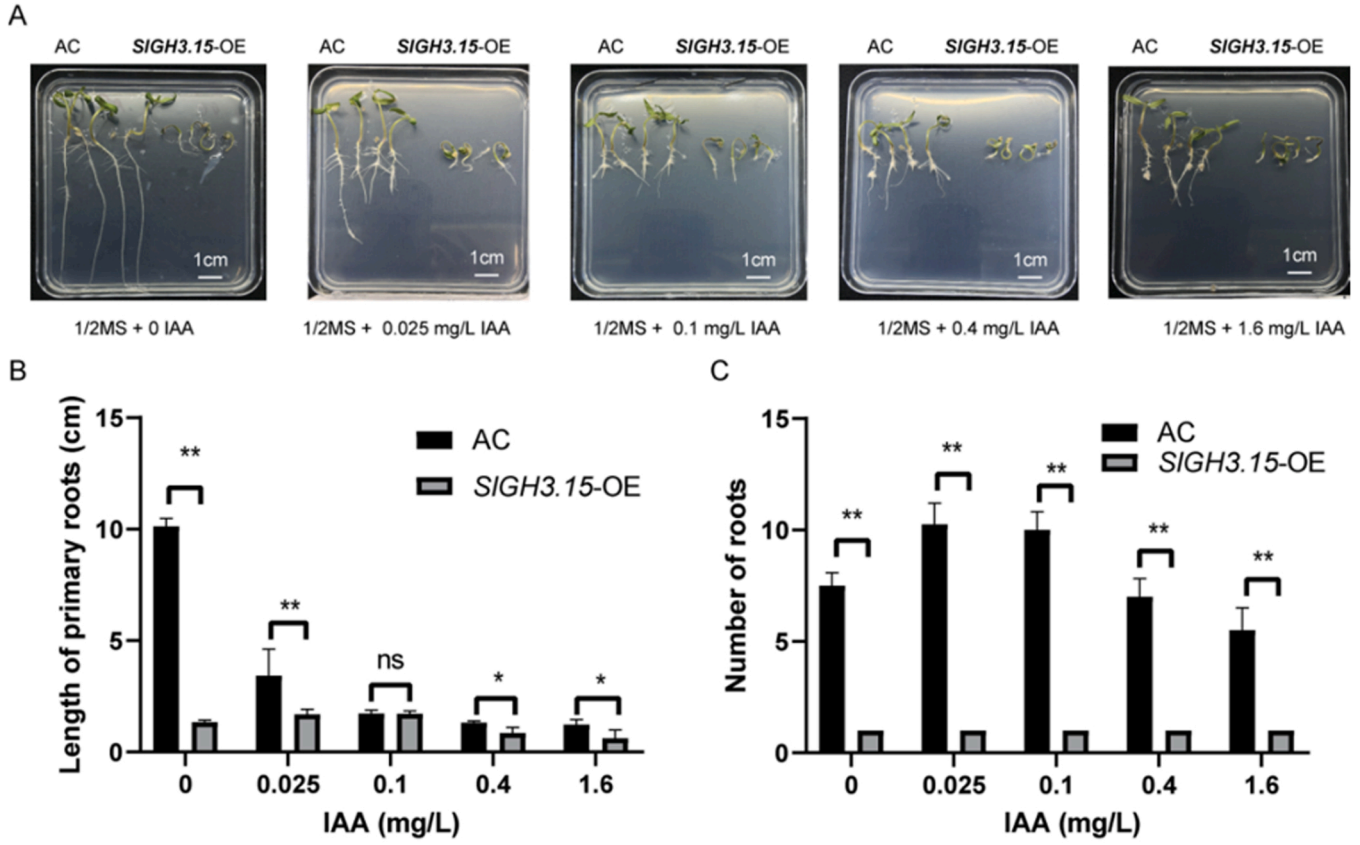

Fig. 5. Reduced insensitivity of root growth to exogenous IAA treatment in transgenic tomato plants overexpressing *SlGH3.15*. (A) Root phenotypes in *SlGH3.15*-OE-10 and AC in response to the treatment of different IAA concentrations (n = 4). Seeds of AC control and *SlGH3.15*-OE-10 lines were germinated on ½MS-agar medium containing IAA at 0 mg/L, 0.025 mg/L, 0.1 mg/L, 0.4 mg/L, and 1.6 mg/L. The plates were placed in a growth room in a vertical position for 7 days. Scale bar, 1 cm. (B) Length of the primary roots (cm) in *SlGH3.15*-OE-10 and AC in response to the treatment of different IAA concentrations (n = 4) in Fig. 5A. (C) Lateral roots in *SlGH3.15*-OE-10 and AC in response to the treatment of different IAA concentrations (n = 4) in Fig. 5A. The asterisks indicate significant differences between groups using Student's *t*-tests: * , $P < 0.05$; * *, $P < 0.01$.

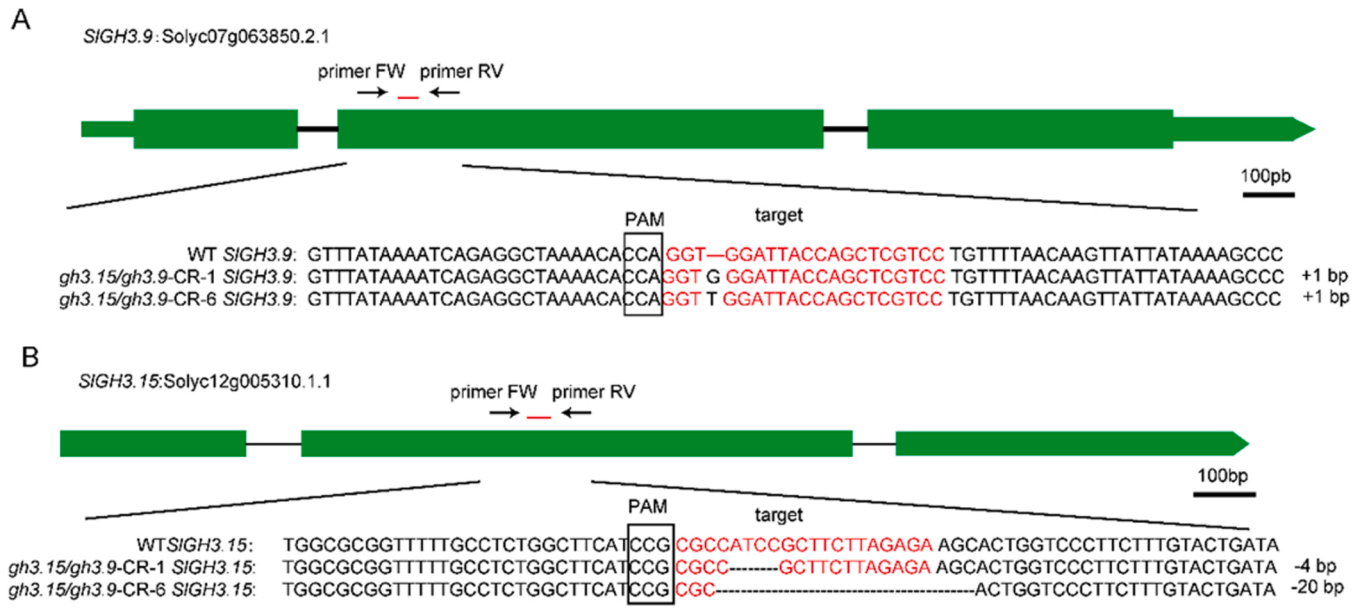

Fig. 6. Generation of *gh3.15/gh3.9* double mutants by CRISPR/Cas9. (A) Schema of the sgRNA target site in *SlGH3.9*. Two black arrows stand for the PCR genotyping primers. *gh3.15/gh3.9*-CR-1 carried a single 1-bp insertion (G) and *gh3.15/gh3.9*-CR-6 carried a single 1-bp insertion (T) resulting in the frame shift. (B) Schema of the sgRNA target site in *SlGH3.15*. Two black arrows refer to the PCR genotyping primers. *gh3.15/gh3.9*-CR-1 carried a single 4-bp deletion and *gh3.15/gh3.9*-CR-6 carried a single 20-bp deletion resulting in the frame shift.

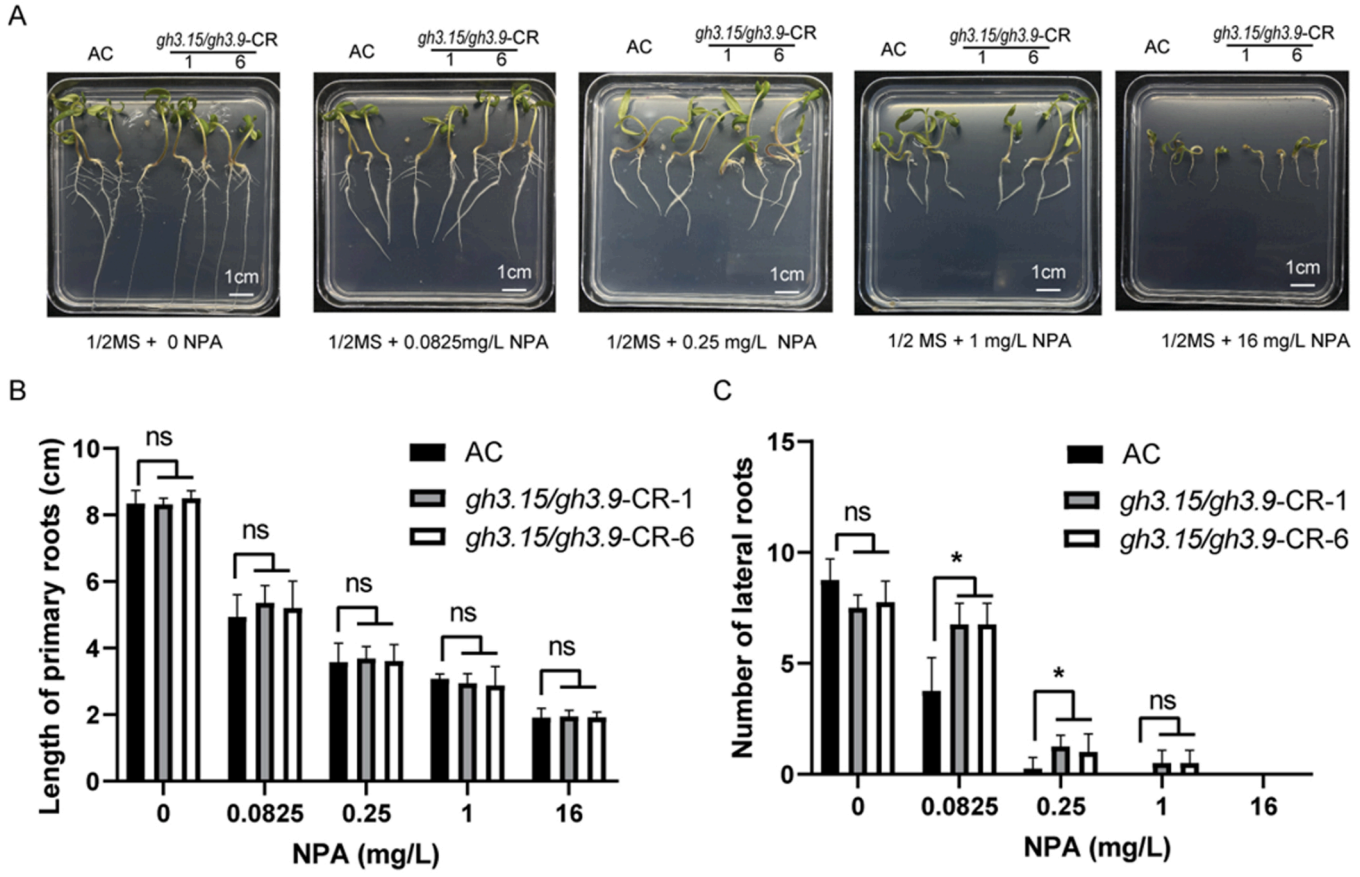

Fig. 7. Reduced sensitivity of roots to NPA treatment in *gh3.15/gh3.9*-CR double mutants. (A) Primary roots in *gh3.15/gh3.9*-CR and AC grown with different concentrations of NPA. Seeds of the double mutants and the control AC were germinated on ½ MS-agar medium containing NPA at the concentrations of 0 mg/L, 0.0825 mg/L, 0.25 mg/L, 1 mg/L, and 16 mg/L. Plates were placed in a growth room in a vertical position for 7 days. Scale bar, 1 cm. (B) length of primary roots in *gh3.15/gh3.9*-CR and AC grown with different concentrations of NPA in Fig. 7A. (C) Lateral roots in *gh3.15/gh3.9*-CR and AC grown at different concentrations of NPA (Fig. 7A). The asterisks indicate significant differences between groups analyzed by using Student's *t*-tests: *, $P < 0.05$; **, $P < 0.01$. ns: no significant.

resistant to the effects of exogenously applied NPA than AC and could produce more lateral roots at a lower NPA concentration. Collectively, our findings implicate *GH3.15* and *GH3.9* in lateral root growth via regulation of auxin homeostasis.

3. Discussion

Functional studies on *GH3* family genes have revealed that they function in cellular auxin homeostasis by conjugating auxin (mostly IAA) to different amino acids in different plant species [Staswick et al., 2005; Nakazawa et al., 2001; Liu et al., 2005; Zhang et al., 2007; Park et al., 2007; Nobuta et al., 2007; Westfall et al., 2012]. There has been limited functional information about the potential functions of these *GH3* genes in tomatoes. This study uncovers the role of *SlGH3.15* in controlling free IAA levels and formation of lateral roots in tomato.

It has been well documented that the changes in cellular auxin concentration, through either external auxin supply or modulation of auxin-related genes, could significantly affect the processes of pathogen infection, plant growth, development, fruit ripening, metabolism, organogenesis, and arbuscular mycorrhizal (AM) colonization in plants (Nakazawa et al., 2001; Takase et al., 2004; Park et al., 2007; Hanlon and Coenen, 2011; Serrani et al., 2008; Etemadi et al., 2014; Hu et al., 2017; Wang et al., 2018). *SlGH3.15* was shown to be involved in controlling the amount of free IAA in tomato. *SlGH3.15* overexpression in transgenic plants decreased free IAA levels (Fig. 3). Plants of the *SlGH3.15*-OE lines showed severely abnormal defects in the vegetative development (Fig. 2), suggesting that a reduction in free IAA content has severe effects on plant growth. The powerful function of *SlGH3.15* in the regulation of free IAA content could potentially be applied for the control of IAA in transgenic plants (Fig. 5). The observations described in this report are of physiological relevance and could provide an explanation for the dwarfism phenotype of the *SlGH3.15*-OE plants, connecting the arrested growth of plants with the phytohormonal shortage.

Besides, the results of the reduced contents of free IAA in tomato leaves of the *SlGH3.15*-OE plants suggest that *SlGH3.15* is involved in IAA homeostasis. Additionally, it is intriguing to note that the exogenous IAA supply could partially restore the defects in the *SlGH3.15*-OE plants. Previous studies have shown that gravity influences the root architecture, which in turn affects structural support and water and nutrient absorption. The gravitropic perception is a fundamental plant biology subject, which has been extensively studied in *Arabidopsis* (Su et al., 2017; Sato et al., 2015; Rashotte et al., 2000). The root cap senses the gravity, leading to the redistribution of PIN proteins in the root cap and the changes of auxin levels in roots. The dramatic reduction in free IAA contents in the *SlGH3.15*-OE plants may result in the lack of sufficient auxin for PIN proteins to transport. Exogenous IAA supply added free IAA to the plant cells and allowed PIN proteins to perform polar transport. Therefore, the phenotype of geotropism in *SlGH3.15*-OE lines was partially rescued by exogenous IAA. In addition, the overexpression of *SlGH3.15* resulted in formation of crimped leaves (Fig. 2D), with a high expression pattern of *SlGH3.15* in leaves (Fig. 1B), thus indicating a significant role of *SlGH3.15* in free IAA homeostasis in vegetative growth. In a previous report, enhanced expression of *AtGH3.6*, an orthologous gene of *SlGH3.15,* has been found to have no effect on the free IAA levels, but to increase the level of IAA-Asp conjugate in *Arabidopsis* (Staswick et al., 2005). Thus, distinct mechanisms may account for regulation of auxin homeostasis in tomato and *Arabidopsis*.

Both monocotyledons and dicotyledons rely heavily on lateral root development for their root architecture (Petricka et al., 2012; Peret et al., 2009). As a dicotyledon, *Arabidopsis* has a single, primary root and develops continuous branches to generate the lateral roots (Osmont et al., 2007). IAA has been found in multiple studies to significantly influence plant root development, specifically in lateral root formation (Bhalerao et al., 2002; Buer and Muday, 2005; Sukumar et al., 2013; Gutierrez et al., 2012; Zhao and Xue, 2020). In our study, we found that exogenous IAA reduced the length of the primary root and increased the number of lateral roots. Reduced lateral root development was a direct result of the increased expression of *SlGH3.15*. Additionally, the *SlGH3.15*-RNAi lines and the control plants were not distinguishable from one another in terms of overall plant size and root development (Fig. 2), implying the redundancy of gene functions. The changed expression of *GH3.9* in *SlGH3.15*-OE lines also showed the possibility of functional redundancy. Therefore, we generated the double mutant *gh3.15/gh3.9*-CR lines in subsequent experiments. We applied the exogenous NPA to the double mutant *gh3.15/gh3.9*-CR lines, the results showed that the double mutant *gh3.15/gh3.9*-CR lines exhibited diminished sensitivity to the NPA treatment, indicating the redundant function of *GH3.15* in root development.

Previous studies have shown that the *SlGH3.15* locus is physically close to a domestication sweep in the tomato genome (Lin et al., 2014). However, enhancing the expression of *SlGH3.15* showed abnormal architectures of the plant (Fig. 2) and loss of the normal ability to bear fruits (Fig. 2), implying the indirect function of *SlGH3.15* in the control of fruit weight in tomato.

In conclusion, the results of this study show that *SlGH3.15*, along with *SlGH3.9*, plays a crucial role in the maintenance of free IAA through the modulation of auxin homeostasis in tomato. As a member of the *GH3* gene family, *SlGH3.15* plays a crucial role in the regulation of plant growth and development in tomato.

4. Materials and methods

4.1. Plant materials

Alisa Craig (AC) cultivars of tomato (*Solanum lycopersicum*) were employed as both the wild-type control and the target for plant transformation. Seeds were germinated and cultivated to maturity in a greenhouse. The relative gene expression and free IAA concentrations were evaluated in the young leaves of 7-week-old seedlings. Root phenotypic experiments were performed by sowing seeds on ½ Murashige-Skoog (MS)-agar media and then transferred them to ½ MS media with various concentrations of IAA or NPA.

4.2. Plasmid construction and plant transformation

Primers based on the sequence of *Solyc12g005310* in the SGN website (https://solgenomics.net/) were used to amplify the *SlGH3.15* CDS from a cDNA pool representing many tissues. For recombination-based gene cloning, gene primers were fused to the attB1 and attB2 sites. Both the pDONR221 and pMV2 vectors (both derived from pHELLSGATE2) were integrated via BP and LR reactions (Invitrogen, USA). The pHELLSGATE8 vector contains the cloned *SlGH3.15* RNAi construct. In both vector systems, we used CaMV 35 S promoter to drive the overexpression construct and the RNAi construct, respectively. *SlGH3.15* and *SlGH3.9* sgRNAs were included in the CRISPR/Cas9 vector used to create the double mutant. The method for creating the recombinant vector was modified from previous report (Ye et al., 2017). The primers are detailed in the supplementary materials (Table S1).

Tomato cultivar AC was transformed using the constructs and *Agrobacterium tumefaciens* strain C58 for the transformation. Transgenic plants were screened by kanamycin selection media and confirmed by amplification the target sequences using gDNA of plants as a template with vector forward and gene-specific reverse primers.

4.3. Subcellular localization

The *SlGH3.15* cDNA's complete coding region (CDS) was in-frame fused to the YFP coding sequence under the CaMV 35 S promoter to facilitate *SlGH3.15* subcellular localization. Five-week-old *Nicotiana benthamiana* plants had this construct injected into their leaf tissues after being transformed with the *Agrobacterium tumefaciens* strain, GV3101. After 48 h of Agrobacterium penetration, the YFP fluorescence was

visualized with a double focusing scanning microscope.

4.4. Quantitative real-time PCR

Trizol reagents (Invitrogen, USA) were used to extract total RNA in accordance with the manufacturer's protocol. After removing the genomic DNA from the RNA samples, the samples were processed with RNase-free DNase I (Invitrogen, USA). First-strand cDNA was synthesized from 3 μl of total RNA using reverse transcriptase and oligo dT (vazyme, http://www.vazyme.com/). Before the quantitative real-time polymerase chain reaction, the cDNA products were diluted as the template of subsequent experiments. Primers for the qRT-PCR were designed with an online primer design website, Primer quest (http://www.idtdna.com/Scitools/Applications/Primerquest/). qRT-PCR was performed using the QuantStudio (TM) 6 Flex System instrument with the 384-well plate (Applied Biosystems, Thermofisher, USA). There was 4.2 μl of cDNA sample, 5 μl of SYBR mix, and 0.8 μl of gene-specific primers at 10 μM in a total volume of 10 μl in each reaction. The heat cycle included 95 °C for 60 s, followed by 45 repetitions of 57 °C for 20 s, 95 °C for 10 s, and 72 °C for 10 s. The samples were triplicated. Primers, Actin_Fw and Actin_Rv were utilized to analyze the tomato Actin gene (*Solyc11g005330.1.1*) and served as an internal control. The $2^{-\Delta\Delta CT}$ method (Livak and Schmittgen, 2001)was used to compute qRT-PCR data. Table S1 provides a list of primers.

4.5. Quantification of free IAA

Each batch of frozen leaves (about 100 mg) was pounded into a fine powder with liquid nitrogen and free IAA was extracted according to the protocol (Liu et al., 2012). Each sample was weighed, then placed in a 1.5 mL tube, and then combined with 750 μl extraction buffer. The mixtures are placed into ices on a shaking bed for overnight at 4 °C in the dark for at least 16 h and centrifuged at 13,000 rpm for 15 min at 4 °C. After carefully transferring the supernatant to a fresh 1.5 mL tube, the pellet was mixed with 400 L extraction buffer, agitated for 4 h at 4 °C, and centrifuged at 13,000 rpm. With the help of a syringe, we mixed the two supernatants and filtered them using a 0.22-μm pore nylon filter with a 13-mm diameter. After dissolving the filtrate in 200 μl methanol, it was air-dried for about 4 h at room temperature under a stream of nitrogen gas. Liquid chromatography (Liu et al., 2012) was used to analyze the levels of free IAA in the samples.

4.6. Quantification of root gravity response

To assess the root gravitropic responses of plants, we measured the angles of root apices between the horizontal line and the line from the root base to the root apex as illustrated in Fig. S5.

4.7. Data analyses

The R statistical software was used to conduct pair-wise Student's *t*-tests to determine statistically significant differences ($p < 0.05$ and $p < 0.01$) between the control and sample treatments.

CRediT authorship contribution statement

J.Z., G.A. and R.H. planned and designed the research; G.A. and R.H. performed most of the experiments; G.A., R.H. and D.Z. analyzed the data; M.L. generated the *GH3.15*-OE lines. G.A., R.H., G.L. and W.L. conducted greenhouse work; G.A. and R.H. wrote the manuscript; J.Z., J.A., Y.W. and Z.H. revised the manuscript.

Declaration of Competing Interest

The authors declare that they have no known competing financial interests or personal relationships that could have appeared to influence the work reported in this paper.

Data availability

All data supporting the results of this study can be found in this paper or in the supplementary materials.

Acknowledgments

This work was supported by the earmarked fund for China Agricultural Research System (CARS-23-A13) and Guangxi Science and Technology Project (Guike AA22068088).

Appendix A. Supporting information

Supplementary data associated with this article can be found in the online version at doi:10.1016/j.plantsci.2023.111638.

References

L. Abas, M. Kolb, J. Stadlmann, D.P. Janacek, K. Lukic, C. Schwechheimer, L.A. Sazanov, L. Mach, J. Friml, U.Z. Hammes, Naphthylphthalamic acid associates with and inhibits PIN auxin transporters, Proc. Natl. Acad. Sci. U. S. A. 118 (2021).
R.P. Bhalerao, J. Eklof, K. Ljung, A. Marchant, M. Bennett, G. Sandberg, Shoot-derived auxin is essential for early lateral root emergence in Arabidopsis seedlings, Plant J. 29 (2002) 325–332.
C. Boettcher, R.A. Keyzers, P.K. Boss, C. Davies, Sequestration of auxin by the indole-3-acetic acid-amido synthetase GH3-1 in grape berry (Vitis vinifera L.) and the proposed role of auxin conjugation during ripening, J. Exp. Bot. 61 (2010) 3615–3625.
C.S. Buer, G.K. Muday, The transparent testa4 mutation prevents flavonoid synthesis and alters auxin transport and the response of Arabidopsis roots to gravity and light, Plant Cell 17 (2005).
Q.F. Chen, C.S. Westfall, L.M. Hicks, S.P. Wang, J.M. Jez, Kinetic basis for the conjugation of auxin by a GH3 family indole-acetic acid-amido synthetase, J. Biol. Chem. 285 (2010) 29780–29786.
C. Domingo, F. Andres, D. Tharreau, D.J. Iglesias, M. Talon, Constitutive expression of OsGH3.1 reduces auxin content and enhances defense response and resistance to a fungal pathogen in rice, Mol. Plant. Microbe Interact. 22 (2009) 201–210.
M. Etemadi, C. Gutjahr, J.M. Couzigou, M. Zouine, D. Lauressergues, A. Timmers, C. Audran, M. Bouzayen, G. Becard, J.P. Combier, Auxin perception is required for arbuscule development in arbuscular mycorrhizal symbiosis, Plant Physiol. 166 (2014) 281–294.
M. Exposito-Rodriguez, A.A. Borges, A. Borges-Perez, M. Hernandez, J.A. Perez, Cloning and biochemical characterization of ToFZY, a tomato gene encoding a flavin monooxygenase involved in a tryptophan-dependent auxin biosynthesis pathway, J. Plant Growth Regul. 26 (2007) 329–340.
J. Friml, E. Benkova, I. Blilou, J. Wisniewska, T. Hamann, K. Ljung, S. Woody, G. Sandberg, B. Scheres, G. Jurgens, K. Palme, AtPIN4 mediates sink-driven auxin gradients and root patterning in Arabidopsis, Cell 108 (2002) 661–673.
L. Gutierrez, G. Mongelard, K. Flokova, D.I. Pacurar, O. Novak, P. Staswick, M. Kowalczyk, M. Pacurar, H. Demailly, G. Geiss, C. Bellini, Auxin controls Arabidopsis adventitious root initiation by regulating jasmonic acid homeostasis, Plant Cell 24 (2012) 2515–2527.
G. Hagen, T. Guilfoyle, Auxin-responsive gene expression: genes, promoters and regulatory factors, Plant Mol. Biol. 49 (2002) 373–385.
M.T. Hanlon, C. Coenen, Genetic evidence for auxin involvement in arbuscular mycorrhiza initiation, N. Phytol. 189 (2011) 701–709.
W. Hu, S. Fagundez, L. Katin-Grazzini, Y.J. Li, W. Li, Y.N. Chen, X.M. Wang, Z.N. Deng, S. X. Xie, R.J. McAvoy, Y. Li, Endogenous auxin and its manipulation influence in vitro shoot organogenesis of citrus epicotyl explants, Hortic. Res. 4 (2017).
J.K. Ishida, T. Wakatake, S. Yoshida, Y. Takebayashi, H. Kasahara, E. Wafula, C. W. Depamphilis, S. Namba, K. Shirasu, Local auxin biosynthesis mediated by a YUCCA flavin monooxygenase regulates haustorium development in the parasitic plant Phtheirospermum japonicum, Plant Cell 28 (2016) 1795–1814.
S. Khan, J.M. Stone, Arabidopsis thaliana GH3.9 influences primary root growth, Planta 226 (2007a) 21–34.
S. Khan, J.M. Stone, Arabidopsis thaliana GH3.9 in Auxin and Jasmonate Cross Talk, Plant Signal. Behav. 2 (2007b) 483–485.
D.A. Korasick, T.A. Enders, L.C. Strader, Auxin biosynthesis and storage forms, J. Exp. Bot. 64 (2013) 2541–2555.
J.-f Kuang, Y. Zhang, J.-y Chen, Q.-j Chen, Y.-m Jiang, H.-t Lin, S.-j Xu, W.-j Lu, Two GH3 genes from longan are differentially regulated during fruit growth and development, Gene 485 (2011) 1–6.
R. Kumar, P. Agarwal, A.K. Tyagi, A.K. Sharma, Genome-wide investigation and expression analysis suggest diverse roles of auxin-responsive GH3 genes during development and response to different stimuli in tomato (Solanum lycopersicum), Mol. Genet. Genom. 287 (2012) 221–235.

D.R. Lewis, S. Negi, P. Sukumar, G.K. Muday, Ethylene inhibits lateral root development, increases IAA transport and expression of PIN3 and PIN7 auxin efflux carriers, Development 138 (2011) 3485–3495.
D.H. Liao, X. Chen, A.Q. Chen, H.M. Wang, J.J. Liu, J.L. Liu, M. Gu, S.B. Sun, G.H. Xu, The characterization of six auxin-induced tomato GH3 genes uncovers a member, SlGH3.4, strongly responsive to arbuscular mycorrhizal symbiosis, Plant Cell Physiol. 56 (2015) 674–687.
T. Lin, G.T. Zhu, J.H. Zhang, X.Y. Xu, Q.H. Yu, Z. Zheng, Z.H. Zhang, Y.Y. Lun, S. Li, X. X. Wang, Z.J. Huang, J.M. Li, C.Z. Zhang, T.T. Wang, Y.Y. Zhang, A.X. Wang, Y. C. Zhang, K. Lin, C.Y. Li, G.S. Xiong, Y.B. Xue, A. Mazzucato, M. Causse, Z.J. Fei, J. J. Giovannoni, R.T. Chetelat, D. Zamir, T. Stadler, J.F. Li, Z.B. Ye, Y.C. Du, S. W. Huang, Genomic analyses provide insights into the history of tomato breeding, Nat. Genet. 46 (2014) 1220–1226.
H.B. Liu, X.H. Li, J.H. Xiao, S.P. Wang, A convenient method for simultaneous quantification of multiple phytohormones and metabolites: application in study of rice-bacterium interaction, Plant Methods 8 (2012).
K.D. Liu, B.C. Kang, H. Jiang, S.L. Moore, H.X. Li, C.B. Watkins, T.L. Setter, M.M. Jahn, A. GH3-like, gene, CcGH3, isolated from Capsicum chinense L. fruit is regulated by auxin and ethylene, Plant Mol. Biol. 58 (2005) 447–464.
K.J. Livak, T.D. Schmittgen, Analysis of relative gene expression data using real-time quantitative PCR and the 2(-Delta Delta C(T)) Method, Methods 25 (2001) 402–408.
K. Ljung, R.P. Bhalerao, G. Sandberg, Sites and homeostatic control of auxin biosynthesis in Arabidopsis during vegetative growth, Plant J. 28 (2001) 465–474.
J. Ludwig-Mueller, Auxin conjugates: their role for plant development and in the evolution of land plants, J. Exp. Bot. 62 (2011) 1757–1773.
Y. Mano, K. Nemoto, The pathway of auxin biosynthesis in plants, J. Exp. Bot. 63 (2012) 2853–2872.
K. Mashiguchi, K. Tanaka, T. Sakai, S. Sugawara, H. Kawaide, M. Natsume, A. Hanada, T. Yaeno, K. Shirasu, H. Yao, P. McSteen, Y.D. Zhao, K. Hayashi, Y. Kamiya, H. Kasahara, The main auxin biosynthesis pathway in Arabidopsis, Proc. Natl. Acad. Sci. U. S. A. 108 (2011) 18512–18517.
L. Minglin, Y.X. Zhang, T.Y. Chai, Identification of genes up-regulated in response to Cd exposure, in Brassica juncea L, Gene 363 (2005) 151–158.
M. Nakazawa, N. Yabe, T. Ichikawa, Y.Y. Yamamoto, T. Yoshizumi, K. Hasunuma, M. Matsui, DFL1, an auxin-responsive GH3 gene homologue, negatively regulates shoot cell elongation and lateral root formation, and positively regulates the light response of hypocotyl length, Plant J. 25 (2001) 213–221.
K. Nobuta, R.A. Okrent, M. Stoutemyer, N. Rodibaugh, L. Kempema, M.C. Wildermuth, R.W. Innes, The GH3 acyl adenylase family member PBS3 regulates salicylic acid-dependent Defense responses in Arabidopsis, Plant Physiol. 144 (2007) 1144–1156.
R.A. Okrent, M.C. Wildermuth, Evolutionary history of the GH3 family of acyl adenylases in rosids, Plant Mol. Biol. 76 (2011) 489–505.
K.S. Osmont, R. Sibout, C.S. Hardtke, Hidden branches: developments in root system architecture, Annu. Rev. Plant Biol. 58 (2007) 93–113.
J.-E. Park, J.-Y. Park, Y.-S. Kim, P.E. Staswick, J. Jeon, J. Yun, S.-Y. Kim, J. Kim, Y.-H. Lee, C.-M. Park, GH3-mediated auxin homeostasis links growth regulation with stress adaptation response in Arabidopsis, J. Biol. Chem. 282 (2007) 10036–10046.
B. Peret, B. De Rybel, I. Casimiro, E. Benkova, R. Swarup, L. Laplaze, T. Beeckman, M. J. Bennett, Arabidopsis lateral root development: an emerging story, Trends Plant Sci. 14 (2009) 399–408.
J.J. Petricka, C.M. Winter, P.N. Benfey, Control of Arabidopsis root development, Annu. Rev. Plant Biol. Vol 63 (2012) 563–590.
A.M. Rashotte, S.R. Brady, R.C. Reed, S.J. Ante, G.K. Muday, Basipetal auxin transport is required for gravitropism in roots of arabidopsis, Plant Physiol. 122 (2000) 481–490.
E.M. Sato, H. Hijazi, M.J. Bennett, K. Vissenberg, R. Swarup, New insights into root gravitropic signalling, J. Exp. Bot. 66 (2015) 2155–2165.
J.C. Serrani, O. Ruiz-Rivero, M. Fos, J.L. Garcia-Martinez, Auxin-induced fruit-set in tomato is mediated in part by gibberellins, Plant J. 56 (2008) 922–934.
T. Sravankumar, Akash, N. Naik, R. Kumar, A ripening-induced SlGH3-2 gene regulates fruit ripening via adjusting auxin-ethylene levels in tomato (Solanum lycopersicum L.), Plant Mol. Biol. 98 (2018) 455–469.
P.E. Staswick, I. Tiryaki, M.L. Rowe, Jasmonate response locus JAR1 and several related Arabidopsis genes encode enzymes of the firefly luciferase superfamily that show activity on jasmonic, salicylic, and indole-3-acetic acids in an assay for adenylation, Plant Cell 14 (2002) 1405–1415.
P.E. Staswick, B. Serban, M. Rowe, I. Tiryaki, M.T. Maldonado, M.C. Maldonado, W. Suza, Characterization of an Arabidopsis enzyme family that conjugates amino acids to indole-3-acetic acid, Plant Cell 17 (2005) 616–627.
A.N. Stepanova, J. Robertson-Hoyt, J. Yun, L.M. Benavente, D.Y. Xie, K. DoleZal, A. Schlereth, G. Jurgens, J.M. Alonso, TAA1-mediated auxin biosynthesis is essential for hormone crosstalk and plant development, Cell 133 (2008) 177–191.
A.N. Stepanova, J. Yun, L.M. Robles, O. Novak, W.R. He, H.W. Guo, K. Ljung, J. M. Alonso, The Arabidopsis YUCCA1 flavin monooxygenase functions in the indole-3-pyruvic acid branch of auxin biosynthesis, Plant Cell 23 (2011) 3961–3973.
S.H. Su, N.M. Gibbs, A.L. Jancewicz, P.H. Masson, Molecular mechanisms of root gravitropism, Curr. Biol. 27 (2017) R964–R972.
S. Sugawara, S. Hishiyama, Y. Jikumaru, A. Hanada, T. Nishimura, T. Koshiba, Y. Zhao, Y. Kamiya, H. Kasahara, Biochemical analyses of indole-3-acetaldoximedependent auxin biosynthesis in Arabidopsis, Proc. Natl. Acad. Sci. U. S. A. 106 (2009) 5430–5435.
P. Sukumar, G.S. Maloney, G.K. Muday, Localized induction of the ATP-binding cassette B19 auxin transporter enhances adventitious root formation in Arabidopsis, Plant Physiol. 162 (2013) 1392–1405.
M.H. Sun, H. Li, Y.B. Li, H.Z. Xiang, Y.D. Liu, Y. He, M.F. Qi, T.L. Li, Tomato YABBY2b controls plant height through regulating indole-3-acetic acid-amido synthetase (GH3.8) expression, Plant Sci. 297 (2020).
T. Takase, M. Nakazawa, A. Ishikawa, M. Kawashima, T. Ichikawa, N. Takahashi, H. Shimada, K. Manabe, M. Matsui, ydk1-D, an auxin-responsive GH3 mutant that is involved in hypocotyl and root elongation, Plant J. 37 (2004) 471–483.
W. Teale, K. Palme, Naphthylphthalamic acid and the mechanism of polar auxin transport, J. Exp. Bot. 69 (2018) 303–312.
S. Vanneste, J. Friml, Auxin: a trigger for change in plant development, Cell 136 (2009) 1005–1016.
Y.C. Wang, N. Wang, H.F. Xu, S.H. Jiang, H.C. Fang, M.Y. Su, Z.Y. Zhang, T.L. Zhang, X. S. Chen, Auxin regulates anthocyanin biosynthesis through the Aux/IAA-ARF signaling pathway in apple, Hortic. Res. 5 (2018).
D. Weijers, E. Benkova, K.E. Jager, A. Schlereth, T. Hamann, M. Kientz, J.C. Wilmoth, J. W. Reed, G. Jurgens, Developmental specificity of auxin response by pairs of ARF and Aux/IAA transcriptional regulators, EMBO J. 24 (2005) 1874–1885.
C.S. Westfall, C. Zubieta, J. Herrmann, U. Kapp, M.H. Nanao, J.M. Jez, Structural Basis for Prereceptor Modulation of Plant Hormones by GH3 Proteins, Science 336 (2012) 1708–1711.
C. Won, X.L. Shen, K. Mashiguchi, Z.Y. Zheng, X.H. Dai, Y.F. Cheng, H. Kasahara, Y. Kamiya, J. Chory, Y.D. Zhao, Conversion of tryptophan to indole-3-acetic acid by TRYPTOPHAN AMINOTRANSFERASES OF ARABIDOPSIS and YUCCAs in Arabidopsis, Proc. Natl. Acad. Sci. U. S. A. 108 (2011) 18518–18523.
A.W. Woodward, B. Bartel, Auxin: regulation, action, and interaction, Ann. Bot. 95 (2005) 707–735.
J. Ye, X. Wang, T.X. Hu, F.X. Zhang, B. Wang, C.X. Li, T.X. Yang, H.X. Li, Y.G. Lu, J. J. Giovannoni, Y.Y. Zhang, Z.B. Ye, An InDel in the promoter of Al-ACTIVATED MALATE TRANSPORTER9 selected during tomato domestication determines fruit malate contents and aluminum tolerance, Plant Cell 29 (2017) 2249–2268.
Z. Zhang, Q. Li, Z. Li, P.E. Staswick, M. Wang, Y. Zhu, Z. He, Dual regulation role of GH3.5 in salicylic acid and auxin signaling during Arabidopsis-Pseudomonas syringae interaction, Plant Physiol. 145 (2007) 450–464.
C.Y. Zhao, H.W. Xue, PI4Kgamma2 interacts with E3 ligase MIEL1 to regulate auxin metabolism and root development, Plant Physiol 184 (2020) 933–944.
Y.D. Zhao, Auxin biosynthesis: a simple two-step pathway converts tryptophan to indole-3-acetic acid in plants, Mol. Plant 5 (2012) 334–338.